Supporting Information

Mixed Copper States in Anodized Cu Electrocatalyst for Stable and Selective Ethylene Production from CO_2 Reduction

Si Young Lee[†, ‡], *Hyejin Jung*[†, ‡], Nak-Kyoon Kim[§], Hyung-Suk Oh[†], Byoung Koun Min[†, ǁ], Yun Jeong Hwang*[†, ǂ]

[†]Clean Energy Research Center, Korea Institute of Science and Technology, 5, Hwarang-ro 14-gil, Seongbuk-gu, Seoul, 02792, Republic of Korea

[‡] Division of Energy and Environmental Technology, KIST School, Korea University of Science and Technology, Hwarang-ro 14 gil 5, Seongbuk-gu, Seoul, 02792, Republic of Korea

[§] Advanced Analysis Center, Korea Institute of Science and Technology, 5, Hwarang-ro 14-gil, Seongbuk-gu, Seoul, 02792, Republic of Korea

[ǁ]Green School, Korea University, 145, Anam-ro, Seonbuk-gu, Seoul, 02842, Republic of Korea

*Corresponding author. Tel: +82-2-958-5227. Fax: +82-2-958-5809.

E-mail address: yjhwang@kist.re.kr (Y. J. Hwang)

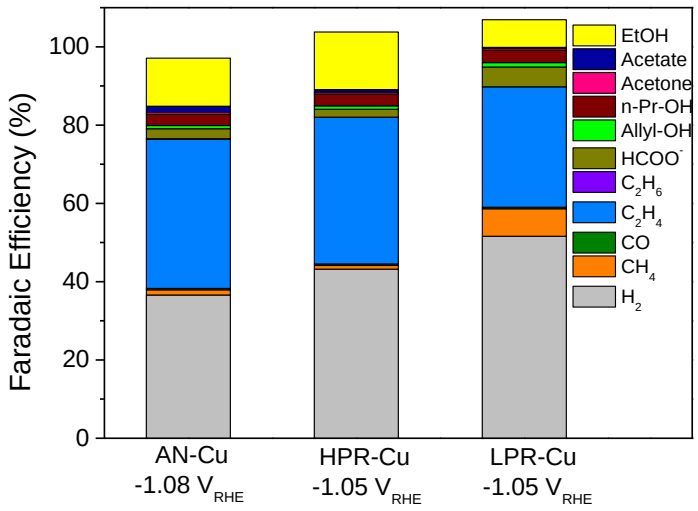

Figure S1. Sum of the Faradaic efficiencies of each gas and liquid products with the AN-Cu and its modified catalysts (HPR-Cu and LPR-Cu) at a fixed potential.

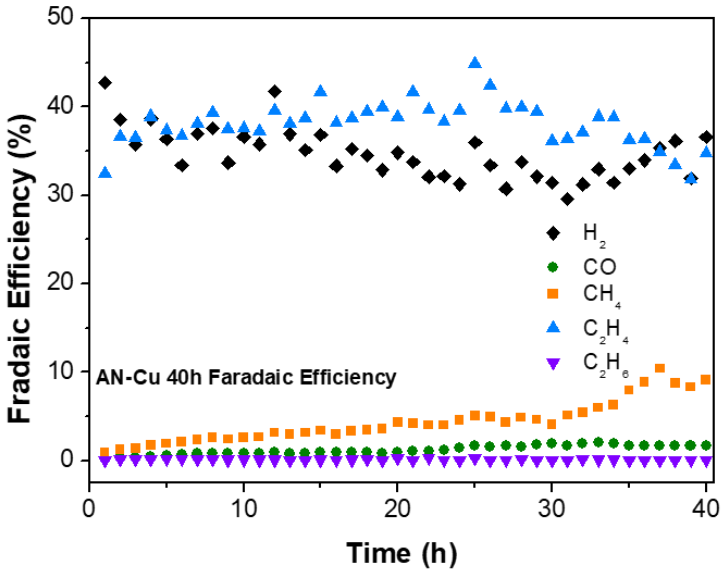

Figure S2. Long-term (40h) bulk electrolysis showing gas product analysis of the AN-Cu catalyst

Table S1. Total amount of the charge flow in reduction step for the preparation of HPR-Cu and LPR-Cu catalysts.

Catalyst	Average Total Charge Flow Density (C/cm^2)
HPR Treat	31.57 ± 0.55
LPR Treat	3.77 ± 0.58

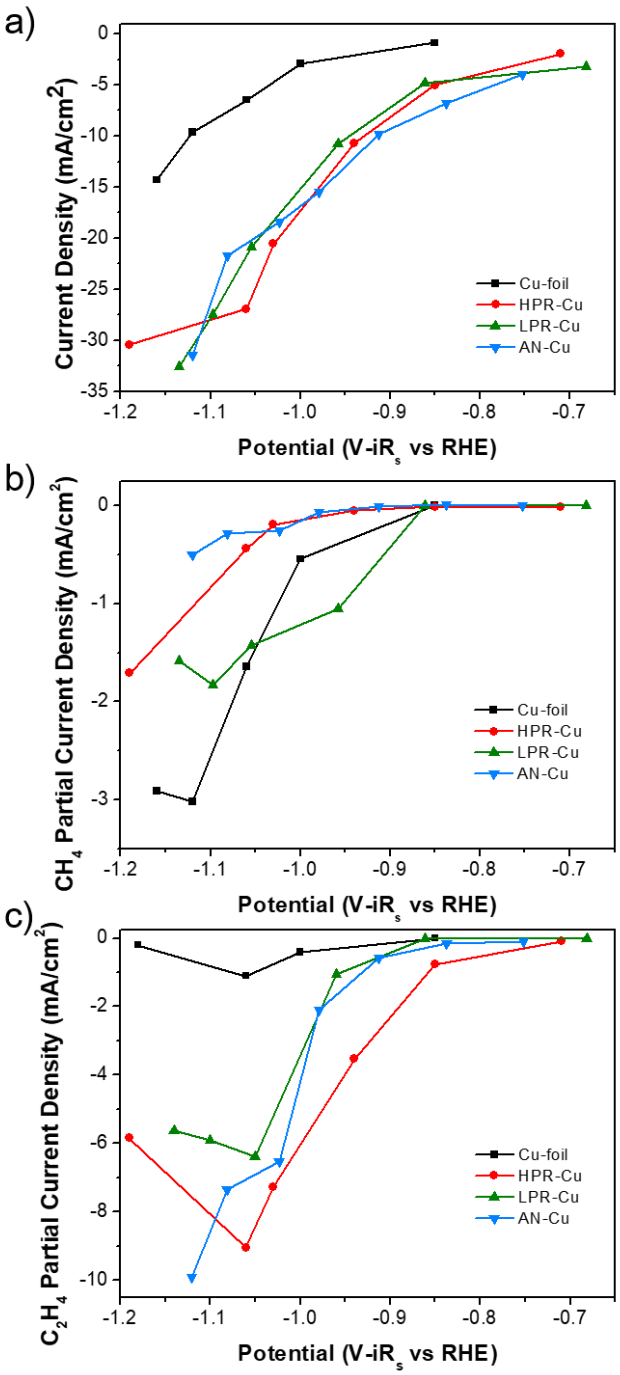

Figure S3. Current density of each Cu electrocatalyst: a) total current density, b) partial current density for CH_4 production, and c) partial current density for C_2H_4 production.

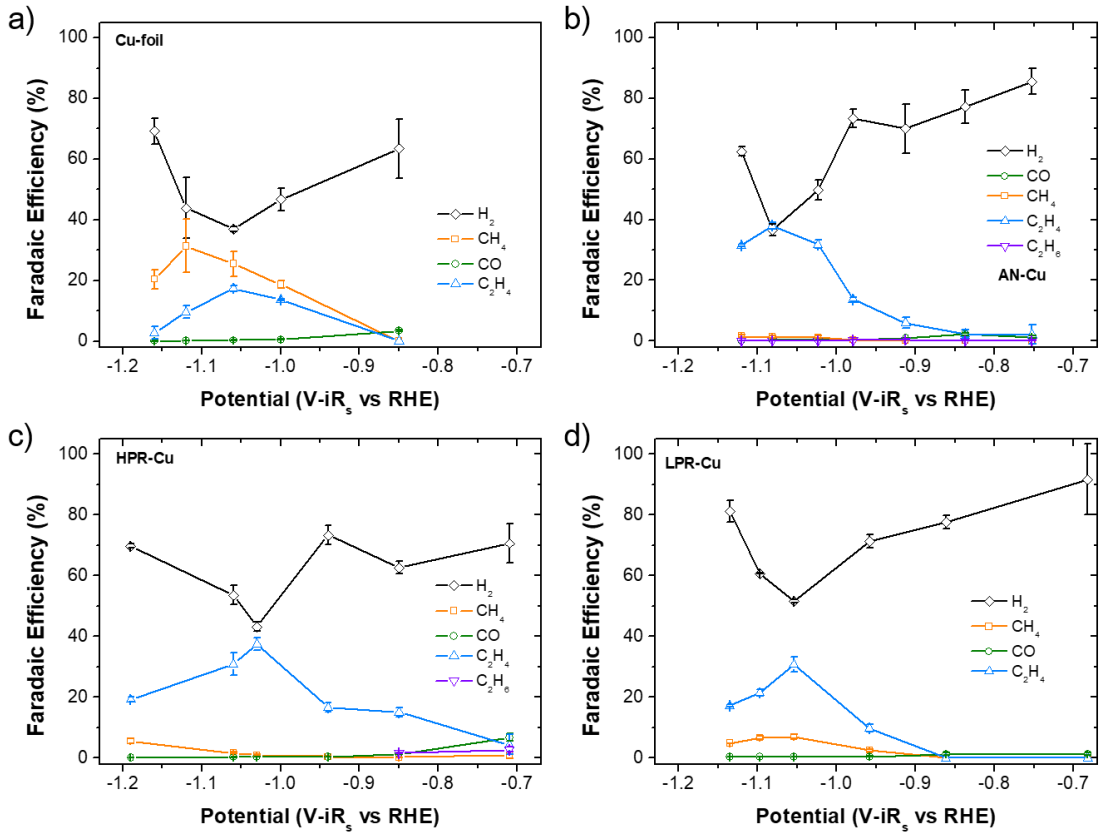

Figure S4. Faradaic efficiency of gas products analyzed at the various applied potentials: a) Cu-foil, b) AN-Cu, c) HPR-Cu, and d) LPR-Cu catalyst.

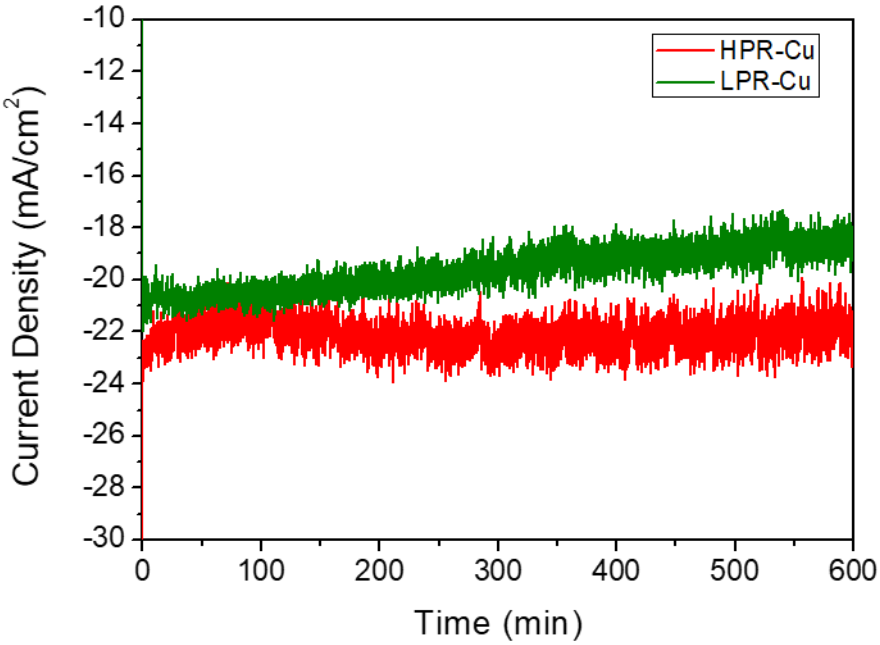

Figure S5. Total current densities of HPR-Cu and LPR-Cu catalysts measured over 10 hour CO_2RR at -1.05 V vs RHE.

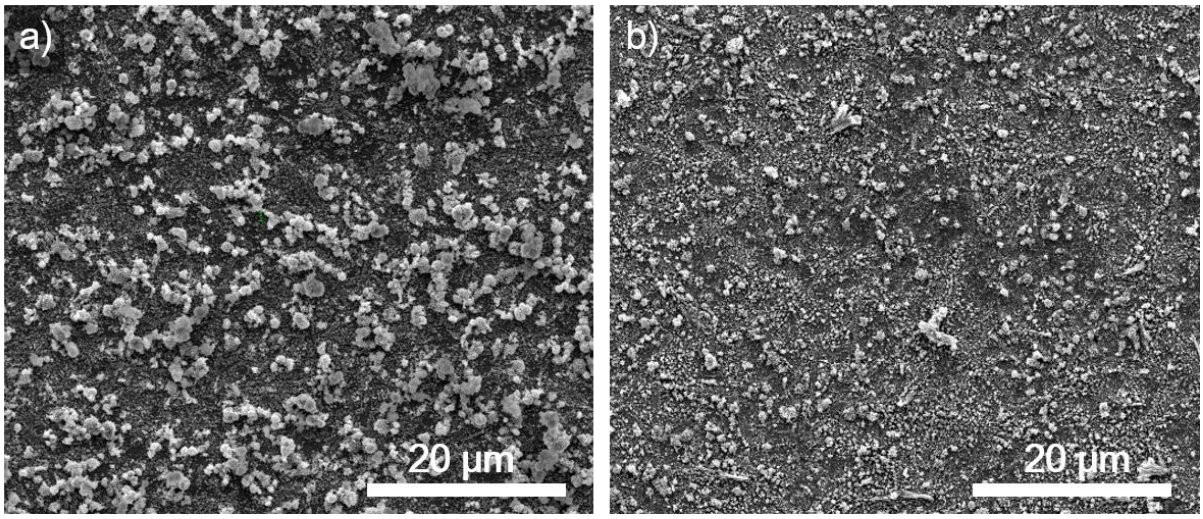

Figure S6. SEM images taken after 100 min of CO_2 RR at -1.05 V vs. RHE: a) HPR-Cu and b) LPR-Cu

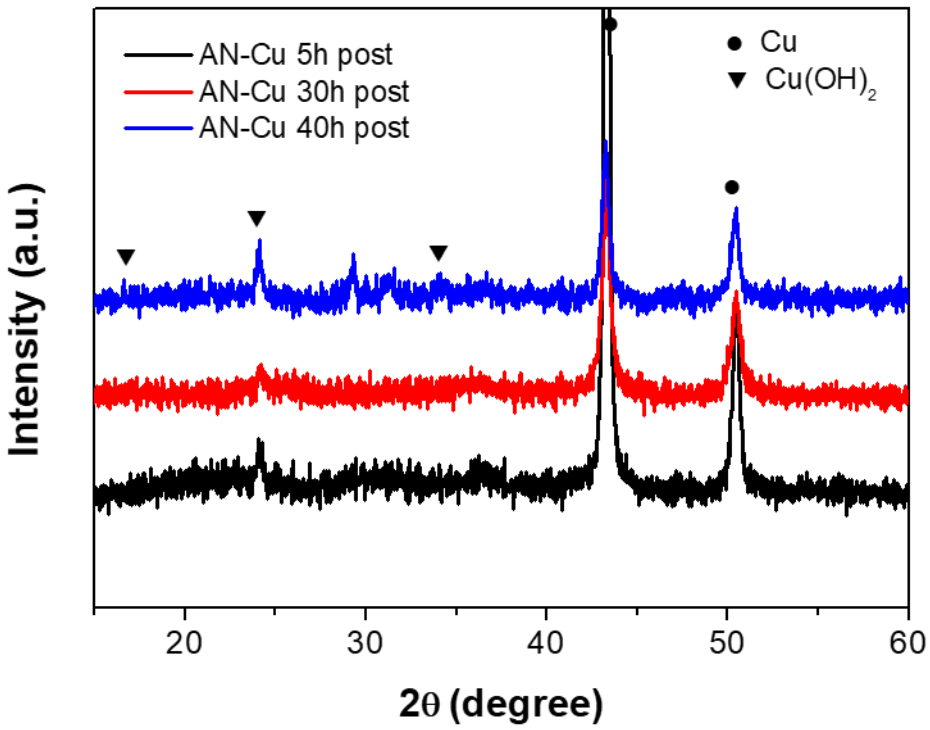

Figure S7. Time dependent GI-XRD analysis of AN-Cu catalyst after 5h, 30h, and 40 h of CO_2 reduction reaction.

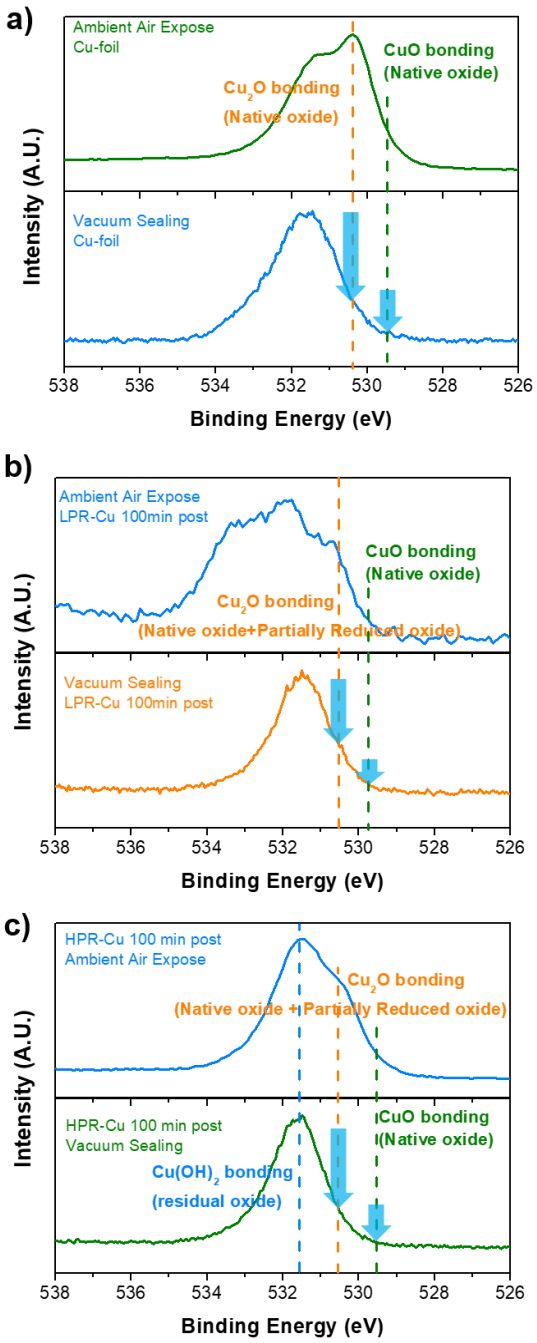

Figure S8. XPS O 1s spectra depending on the sample storage and transfer methods showing inhibition of Cu re-oxidation stored/transferred in vacuum sealing condition compared with in air exposure: a) a flat Cu-foil, b) LPR-Cu CO_2 RR, and c) HPR-Cu CO_2 RR

Table S2. Oxygen and cooper atomic concentration and ratio compared by K-alpha XPS.

Sample	Cu (XPS At %)	O (XPS At%)	O/Cu ratio
AN-Cu	26.61	47.07	1.77
AN-Cu 100min post	22.38	22.85	1.02
HPR-Cu	18.41	21.08	1.15
HPR-Cu 100min post	36.78	20.70	0.55
LPR-Cu	45.67	8.47	0.19
LPR-Cu 100min post	61.76	5.23	0.08

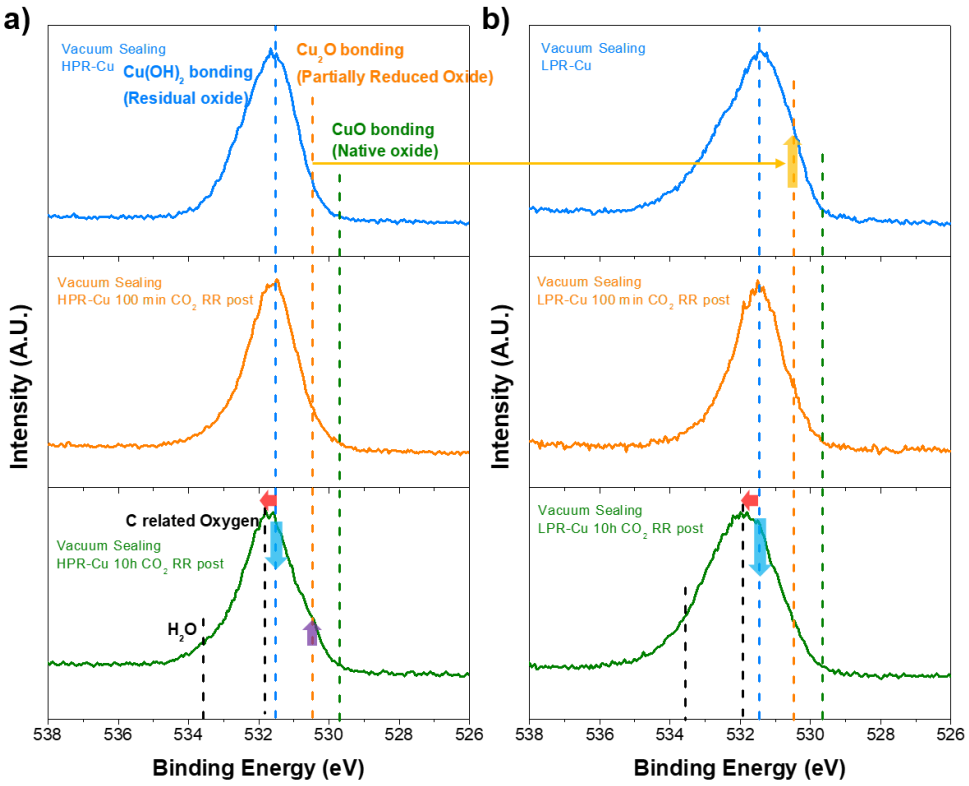

Figure S9. XPS O 1S spectra pre- and post-CO_2RR: a) HPR-Cu and b) LPR-Cu catalysts ($Cu(OH)_2$: 531.5 eV, Cu_2O : 530.5 eV, CuO : 529.8 eV, C related oxygen 531.9 eV, H_2O : 533.5 eV)

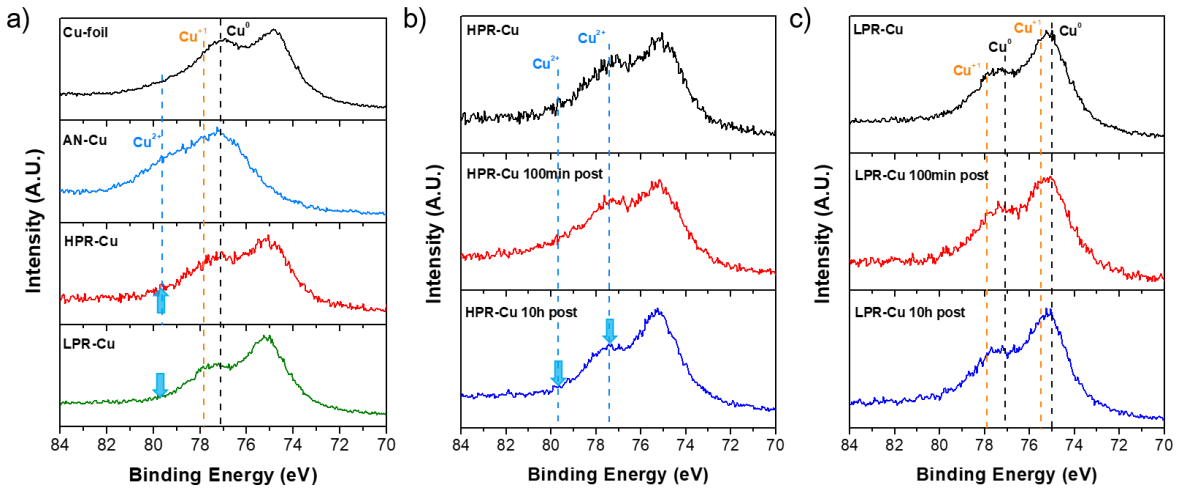

Figure S10. Cu 3p XPS spectra of each Cu based electrocatalyst measured at beam-line at PAL: a) comparison of initial state (before CO_2RR), and Cu 3p XPS spectra changes after 100 min and 10 hours of CO_2RR on b) the HPR-Cu and c) the LPR-Cu.

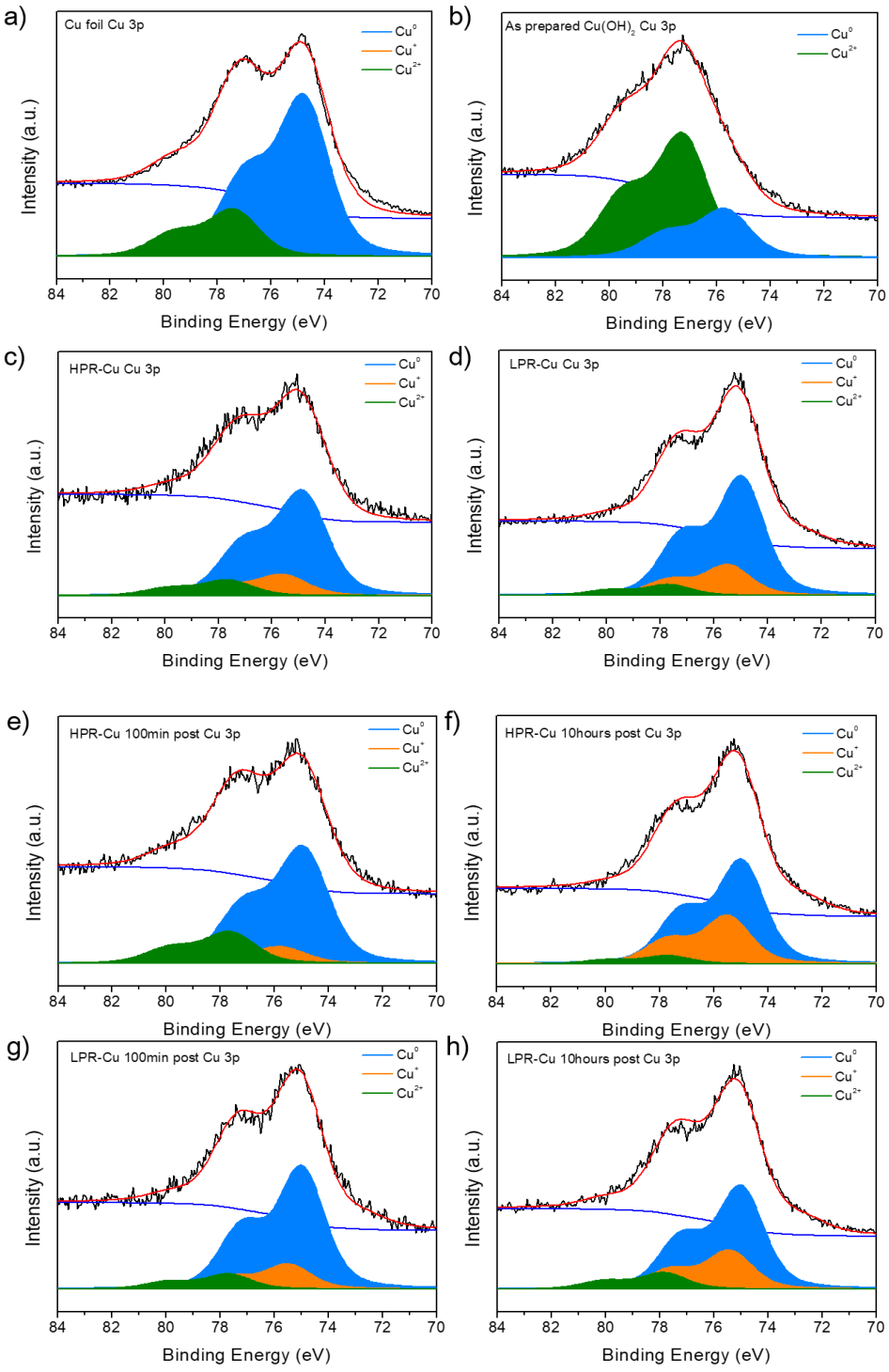

Figure S11. Deconvoluted Cu 3p spectra of each electrocatalyst: a) Cu-foil, b) AN-Cu, c) HPR-Cu, d) LPR-Cu, e) 100min post HPR-Cu, f) 10h post HPR-Cu, g) 100min post LPR-Cu, h) 10h post LPR-Cu